Title: Postpartum breast cancer progression is driven by semaphorin 7a mediated invasion and survival

Running title: PPBC is driven by SEMA7A-mediated invasion and survival

Sarah E Tarullo[1,2], Ryan C Hill[3], Kirk Hansen[3], Fariba Behbod[4], Virginia F Borges[1,2,5], Andrew C Nelson[6], and Traci R Lyons[1,2,5]*

Affiliations:
[1]Department of Medicine, Division of Medical Oncology, CU Anschutz Medical Campus, Aurora, CO 80045

[2]Young Women's BC Translational Program, CU Anschutz Medical Campus, Aurora, CO 80045

[3]Department of Biochemistry and Molecular Genetics, CU Anschutz Medical Campus, Aurora, CO 80045

[4]Division of Cancer and Developmental Biology, University of Kansas Medical Center, Kansas City, KS 66160

[5]University of Colorado Cancer Center, Aurora, CO 80045

[6]Department of Laboratory Medicine and Pathology, University of Minnesota, Minneapolis, MN 55455

***Corresponding Author:** Traci R Lyons (303-724-3885; traci.lyons@cuanschutz.edu)

Conflict of Interest: The authors have declared that no conflict of interest exists.

ABSTRACT:

Young women diagnosed with breast cancer (BC) have poor prognosis due to increased rates of metastasis. Additionally, women within 10 years of most recent childbirth at diagnosis are ~3 times more likely to develop metastasis than age and stage matched nulliparous women. We define these cases as postpartum BC (PPBC) and propose that the unique biology of the postpartum mammary gland drives tumor progression. Our published results revealed roles for SEMA7A in breast tumor cell growth, motility, invasion, and tumor associated-lymphangiogenesis, all of which are also increased in pre-clinical models of PPBC. However, whether SEMA7A drives progression in PPBC remains largely unexplored. Our results presented herein show that silencing of SEMA7A decreases tumor growth in a model of PPBC while overexpression is sufficient to increase growth in nulliparous hosts. Further, we show that SEMA7A promotes multiple known drivers of PPBC progression including tumor associated COX-2 expression and fibroblast-mediated collagen deposition in the tumor microenvironment. Additionally, we show for the first time that SEMA7A expressing cells deposit fibronectin to promote tumor cell survival. Finally, we show that co-expression of SEMA7A/COX-2/FN predicts for poor prognosis in breast cancer patient cohorts. These studies suggest SEMA7A as a key mediator of BC progression and that targeting SEMA7A may open avenues for novel therapeutic strategies.

50 **INTRODUCTION**:

51 Postpartum breast cancer (PPBC), or breast cancers (BC) diagnosed within 5-10
52 years of last childbirth, are ~three times more likely to become metastatic [1-3].
53 Specifically, PPBC patients exhibit distant metastasis free five-year survival (DMFS)
54 rates as low as 70% [1], which are further decreased to 50% after ten years [2].
55 Additionally, PPBC may account over half of BCs diagnosed in women aged <45 [1]. In
56 a pre-clinical model of PPBC a non-metastatic BC cell line becomes invasive and
57 metastatic upon orthotopic implantation at the onset of postpartum mammary gland
58 involution [4]. Postpartum/post-lactational mammary involution returns the gland to the
59 pre-pregnant state; we and others have shown that programs associated with
60 postpartum involution are similar to tumor-promotional microenvironments [1, 4-9].
61 Since the MCF10DCIS model initially resembles ductal carcinoma in situ (DCIS), which
62 progresses to ER/PR/HER2 negative invasive ductal carcinoma (IDC) [10], we utilized
63 this model to show accelerated tumor growth and progression to IDC in postpartum
64 hosts [4]. This progression was driven by collagen deposition and expression of
65 cyclooxygenase-2 (COX-2), both of which were required for tumor cell invasion.
66 Additionally, a weakly tumorigenic breast epithelial cell line, HMLE-Ras^{lo}, was similarly
67 promoted via host driven mechanisms [11]. More recently, expression of a neuronal
68 guidance molecule, Semaphorin 7a (SEMA7A), was observed in mouse mammary
69 epithelium during postpartum involution and in the tumors that outgrew after
70 implantation during involution [6].

71 Semaphorins are characterized for their roles during development, however and
72 have reported roles in multiple cancer types [12-16] and SEMA7A expression is

73 emerging as poor prognostic indicator [6, 16-20]. SEMA7A can promote cell-
74 autonomous signaling when it remains bound to the cell via its
75 glycosylphosphatidylinositol (GPI) membrane link or non-cell-autonomous signaling
76 when shed via cleavage into the extracellular environment. Here, we show that
77 SEMA7A protein is expressed in DCIS from BC patients, is necessary for postpartum
78 tumor progression in our pre-clinical model, and sufficient to drive tumor progression in
79 nulliparous hosts. We also demonstrate that shed SEMA7A drives collagen deposition
80 in the tumor microenvironment (TME) via upregulation of collagen I mRNA in fibroblasts,
81 which promotes expression of COX-2 and invasion. Furthermore, we propose a cell-
82 autonomous pro-invasive and survival role for SEMA7A that is mediated through
83 fibronectin (FN), epithelial-to-mesenchymal transition (EMT) and downstream pro-
84 survival signaling via phosphorylation of AKT. Additionally, we show that SEMA7A
85 expressing cells exhibit enhanced metastatic capabilities. Finally, our results we
86 demonstrate that a gene signature of SEMA7A, COX-2, and FN1 predicts for poor
87 prognosis for BC patients suggest that SEMA7A merits further studies to develop a
88 novel therapeutic for BC patients.
89

RESULTS

SEMA7A promotes postpartum tumor progression in a mouse model and is expressed in DCIS from patients

The MCF10DCIS model is ideal for monitoring early events in the metastatic cascade, such as the transition from in situ to invasive. To examine whether SEMA7A drives DCIS progression in postpartum/post-lactational hosts, we orthotopically injected MCF10DCIS cells stably expressing a SEMA7A targeted shRNA (SEMA7A-KD) or nontargeting control (Crtl) [18] at involution day 1 (SFigure1A). We observed that silencing of SEMA7A is sufficient to decrease tumor growth in postpartum hosts despite some of the tumors regaining expression of SEMA7A protein (Figure1A; SFigure1B). Harvested tumors (H&E stained sections) were scored for invasion at 5 weeks post-injection, when the majority of postpartum tumors are normally invasive (SFigure1C), and 33% of the SEMA7A-KD were invasive compared to 86% in the controls. Further, 56% of tumors in the SEMA7A-KD group maintained evidence of DCIS versus 12.5% controls (Figure1B). Finally, 11% of tumors in the KD group were DCIS with microinvasion compared to 0% of controls. Collagen-mediated upregulation of COX-2 is a dominant feature that drives invasion in postpartum hosts in the MCF10DCIS model [4]. Consistent with a role for SEMA7A in collagen/COX-2 dependent invasion in postpartum hosts, we observe that fibrillar collagen deposition, by Massan's trichrome stain, and COX-2 expression, by immunohistochemistry (IHC) are significantly decreased in SEMA7A-KD tumors (Figure1C&D).

To determine whether SEMA7A expression was higher in DCIS from postpartum patients, we performed IHC on DCIS lesions and adjacent normal breast tissue from

113 women in our BC cohort (Figure2A) and quantitated medium + strong staining to show
114 that DCIS lesions express higher levels of SEMA7A than normal breast tissue
115 (Figure2B,SFigure2A). Then, when separated by parity status, we observe increased
116 SEMA7A in DCIS lesions in both nulliparous and postpartum patients, with a trend
117 toward highest expression in postpartum patients, suggesting that SEMA7A expression
118 may have relevance to all patients with DCIS, but may be particularly relevant to
119 postpartum patients (Figure2B,SFigure2B). Consistent with this, paired analysis
120 between normal and DCIS within each patient revealed that the majority of patients in
121 both the nulliparous and postpartum groups exhibited increased SEMA7A expression in
122 DCIS compared to normal (Figure 2C&D). We confirmed this observation by showing
123 similar data on SEMA7A expression in a tissue microarray consisting of additional
124 normal breast and matched patient samples of DCIS using kidney and placenta as
125 negative and positive controls, respectively (Figure2E-G,SFigure2C). Finally, we also
126 show that SEMA7A mRNA levels are increased in DCIS compared to normal in the
127 METABRIC [21] dataset and that SEMA7A is in the top 11% of upregulated genes in
128 DCIS compared normal (p=0.002)(SFigure2D). Taken together, our results suggest that
129 SEMA7A may represent a general mediator of DCIS growth and invasion in both parous
130 and nulliparous women.

131 To test our hypothesis that SEMA7A expression is sufficient to drive DCIS
132 progression, we injected MCF10DCIS cells that overexpress SEMA7A protein
133 (SEMA7A-OE), along with controls, into a separate cohort of nulliparous hosts; we
134 observed accelerated growth of SEMA7A-OE tumors (Figure3A). These tumors were
135 similarly scored for invasion, but at three weeks post-injection, when tumors are

136 normally DCIS in nulliparous hosts (SFigure1C). While, control tumors were all DCIS, as
137 expected, greater than 50% of the SEMA7A-OE tumors had microinvasion and/or were
138 mixed IDC+DCIS (Figure3B;SFigure 3). Additionally, levels of collagen and COX-2,
139 which are normally very low in DCIS tumors in nulliparous hosts, are higher in the
140 SEMA7A-OE tumors, which is consistent with a role for SEMA7A in promoting
141 production (Figure3C&D).

142 **SEMA7A promotes tumor cell invasion via matrix deposition and acquisition of**
143 **mesenchymal phenotypes**

144 To model SEMA7A dependent invasion in vitro, we utilized a 3D organoid model
145 with SEMA7A-OE cells suspended in Matrigel or Matrigel+collagen [4]. We found that
146 SEMA7A overexpression was not sufficient to drive increased invasion on Matrigel
147 alone but sufficient when collagen I was present in the matrix (Figure4A&B). We then
148 validated the requirement for both collagen and SEMA7A in invasion via knockdown in
149 the MDA-MB-231 cell line, which requires collagen for 3D organoid formation [22]
150 (SFigure4A, Figure4C). Since fibroblasts in the TME produce collagen, we then stained
151 for alpha-smooth muscle actin (αSMA), a marker of activated fibroblasts, but did not
152 observe differences in fibroblast infiltration (SFigure4). These results suggest that
153 SEMA7A does not recruit tumor infiltrating fibroblasts.

154 Alternatively, to determine whether SEMA7A expressing tumor cells promote
155 collagen production by fibroblasts via shedding of SEMA7A, we induced serum starved
156 fibroblasts with conditioned media from our SEMA7A-OE tumor cells, alongside
157 conditioned media from control cells and TGFβ as positive control and examined
158 expression of the *COL1A1* mRNA by qPCR. We focused on *COL1A1* because collagen

159 I is the most abundant collagen in the mammary gland [23]. Conditioned medias from
160 SEMA7A OE cells induced *COL1A1* expression in fibroblasts to higher levels than
161 observed in control or TGFβ treated fibroblasts (Figure4D). Then, we treated fibroblasts
162 with purified SEMA7A to show specific induction of COL1A1 gene expression
163 (Figure4E). To understand additional SEMA7A mediated changes to the TME, we
164 performed an unbiased mass spectrometry analysis of conditioned medias from ex vivo
165 tumors derived from SEMA7A-KD or control cells. When we restricted our analysis to
166 ECM peptides of human origin we observed downregulation of several ECM associated
167 molecules with SEMA7A-KD (SFigure4A), but focused on the significant decrease in
168 fibronectin (FN) (Figure5A) after immunostaining of our tumors confirmed decreased FN
169 expression with SEMA7A-KD (Figure5B&C). As FN is frequently associated with EMT,
170 we examined whether SEMA7A expression is also associated with additional
171 mesenchymal markers. We observed SEMA7A dependent expression of matrix
172 remodeling enzyme, matrix metalloproteinase-2, vimentin, and S100A4, as well as other
173 members of the S100 family of proteins (Figure5D-F;SFigure4B-E), which are all
174 secreted by mesenchymal-like cells [24]. To confirm SEMA7A-dependent
175 mesenchymal-like phenotypes we measured cell aspect ratios with the prediction that
176 epithelial-like cells, due to their cuboidal morphology, would exhibit a ratio of ~1 and
177 ratios >1 would be indicative of mesenchymal-like cells. Our results reveal that the
178 mesenchymal-like MDA-MB-231 cells, exhibit decreased average aspect ratios with
179 SEMA7A-KD (Figure5G). Concordantly, SEMA7A-OE in the MCF10DCIS cells, which
180 are less mesenchymal-like, resulted in increased aspect ratios (Figure5H). Furthermore,
181 immunoblot analysis of MCF10DCIS SEMA7A-OE cells reveals decreased E-cadherin

182 and increased vimentin expression, markers of epithelial and mesenchymal cells,
183 respectively (SFigure5F). Together, our results suggest that SEMA7A promotes cellular
184 invasion via both cell-autonomous and non-cell-autonomous mechanisms of matrix
185 deposition and remodeling.

186 **SEMA7A promotes cell survival via fibronectin, AKT and COX-2**

187 We also observed decreased tumor growth of SEMA7A-KD tumors in vivo but did
188 not see significant changes in proliferation marker Ki67 (SFigure5A). However, we did
189 observe a trend toward increased cleaved-caspase 3, a marker of apoptosis, in
190 SEMA7A-KD tumors with a corresponding decrease in SEMA7A-OE tumors
191 (SFigure5B&C). We also observed increased cell death in SEMA7A-KD cells in culture
192 via a luminescent assay for caspase activity, which we validated in the MDA-MB-231
193 cell line (Figure6A&B). Conversely, decreased cell death was observed in the SEMA7A
194 OE cell in both cell lines (SFigure5D, SFigure5E&F). Additionally, analysis of cell death
195 in real time confirmed that SEMA7A-KD MDA-MB-231 cells exhibit increases in cell
196 death via activation of apoptotic signaling (Figure6C). One known pro-survival
197 mechanism co-opted by tumors to block activation of caspase cleavage is activation of
198 pro-survival kinase AKT [25] and we observed decreased levels of phosphorylated AKT
199 via immunoblot for pS473 in SEMA7A-KD and a corresponding increase in levels in
200 SEMA7A OE cells (Figure6D&SFigure5G). Interestingly, FN signals via integrins, which
201 can activate downstream pro-survival pathways, including AKT [26]. To determine
202 whether add-back of FN could rescue SEMA7A-KD cells from cell death, we KD plated
203 cells FN-, laminin- or collagen-coated plates with control cells on tissue culture plastic
204 for reference. We observed increased cell death in all SEMA7A-KD conditions except

205 when FN was present where we observed levels of cell death were more similar to the
206 Ctrl cells (Figure6E). Thus, we suggest that SEMA7A promotes AKT mediated survival
207 by increasing FN deposition and therefore cellular attachment.

208 Mesenchymal-like tumor cells, known to have high levels of FN, are not as
209 dependent on matrix attachment for survival and can also exhibit resistance to normal
210 programs that mediate cell death including survival in detached or anchorage
211 independent conditions [27]. An initial step of the metastatic cascade involves cell
212 detachment from ECM to facilitate local invasion and access to the vasculature; then,
213 cells in circulation must survive in matrix detached conditions prior to extravasating to
214 seed metastatic sites. To assess a role for SEMA7A in promoting survival in circulation,
215 we forced cellular detachment in vitro and measured cleaved-caspase 3/7 to show that
216 SEMA7A-KD increases cell death while SEMA7A-OE promotes cell survival in detached
217 conditions (Figure6F&G, SFigure5H&I). Interestingly, fibronectin was not sufficient to
218 rescue cell death in suspension suggesting that fibronectin deposition is necessary
219 (data not shown). However, since activation of AKT is a known mediator of COX-2
220 expression [28] we also examined the ability of COX-2 KD cells to survive in detached
221 conditions. Similar to our results in the SEMA7A-KD cells we observe that COX-2
222 knockdown cells exhibit increased cell death in detached conditions, which was not
223 observed in attached conditions (SFigure5J) suggesting that SEMA7A mediated
224 upregulation of AKT signaling, and subsequent expression of COX-2, support cell
225 survival in detached conditions such as those encountered during local invasion and in
226 circulation (Figure 6H).

227 **SEMA7A, COX-2, FN and metastatic potential**

228 To assess whether SEMA7A promotes survival in circulation in vivo, we
229 performed tail vein injections of MDA-MB-231 SEMA7A-KD or Ctrl cells (SFigure6A)
230 and assessed for pulmonary metastasis. Our results reveal a decrease in both the
231 number and average size of metastatic lesions per lung with SEMA7A KD (Figure7A)
232 suggesting that SEMA7A plays a role in survival in circulation, as well as a possible role
233 in seeding and outgrowth of BC metastasis. We have previously published that
234 SEMA7A expression is upregulated in IDC compared to normal and the worst overall
235 survival (OS) was observed in SEMA7A+ER-BC in the METABRIC dataset [18];
236 however, in SEMA7A+ER- BCs we do not observe decreased distant metastasis free
237 survival (DMFS) via KmPlot analysis (SFigure6B). Similarly, although transcripts for
238 COX-2 and FN1 are also upregulated in BC (STable1), neither COX-2 or FN1 are
239 associated with decreased DMFS in ER-BC (SFigure6E&F). However, co-expression of
240 COX-2, SEMA7A, and FN1 increases risk for metastasis in ER-BC patients, with 5 year
241 DMFS rates approaching 70% by both KmPlot and GOBO (Gene expression-based
242 Outcome for Breast cancer Online or GOBO) analysis (Figure7B&C) [1]. We also
243 observed that co-expression of our 3 gene signature significantly associates with
244 decreased DMFS in basal and PAM50 basal subtype tumors using GOBO (SFigure6G-
245 I). Finally, co-expression of SEMA7A with both FN and COX-2 is observed in BCs in the
246 TCGA dataset (Figure6D&E).
247

248 **DISCUSSION**

249 All women experience a transient increase in risk for developing breast cancer
250 after each completed pregnancy [4, 29, 30]. Additionally, patients diagnosed with breast
251 cancer within ten years postpartum comprise nearly 50% of all BCs in women <40 in
252 both US and Norwegian cohorts and these PPBC patients are at high risk for metastatic
253 spread [1, 31]. A recent publication by Welch and Hurst defines the hallmarks of
254 metastasis as motility and invasion, modulation of the microenvironment, plasticity, and
255 colonization [32]. Here, we identify roles for SEMA7A in promotion of metastasis using
256 preclinical models regardless of parity status. Our results suggest that SEMA7A drives
257 one described mechanism of tumor progression pertinent to postpartum women, which
258 is collagen mediated upregulation of COX-2 that drives motility and invasion of DCIS
259 cells. However, our results also suggest that this mechanism of invasion can be driven
260 by SEMA7A in both nulliparous and postpartum hosts suggesting it is not unique to
261 parous patients. Further, we extend our observations and identify a novel cell-
262 autonomous mechanism by which SEMA7A mediates tumor cell survival via stimulation
263 of FN production and activation of pro-survival kinase AKT regardless of the host parity
264 status. We also show that SEMA7A supports tumor cell invasion by stably altering cells
265 to a more mesenchymal phenotype, which promotes cell survival in anchorage-
266 independent conditions to allow for colonization of distant organs. Thus, we suggest that
267 SEMA7A plays a key role in multiple steps toward progression to metastatic disease.
268 We support this claim by showing a that co-expression of COX-2, SEMA7A, and FN
269 correlates with distant metastasis formation in BC patients. We propose a model
270 whereby SEMA7A signaling supports metastatic progression (Figure8).

271 SEMA7A was first identified on lymphocytes and originally designated CDw108
272 [33]. CDw108 was renamed SEMA7A due to its structural similarities with members of
273 the Semaphorin family of proteins best known for their roles in neuronal guidance [34].
274 SEMA7A is the only semaphorin linked to the membrane via a GPI anchor; as such, it
275 can be cleaved to result in shedding of SEMA7A into the extracellular environment,
276 which was shown to promote β1-integrin dependent inflammation and fibrosis [35-41].
277 During fibrosis and in response to TGFβ, SEMA7A activates AKT signaling, which
278 results in upregulation of collagen and FN in a β1-integrin dependent manner [42].
279 While our current studies do not explore a role for β1-integrin, we and others have
280 shown that SEMA7A-β1-integrin binding promotes tumor growth, EMT,
281 migration/invasion, metastasis, and neo-vasculogenesis [17, 19, 20]. Herein, we
282 hypothesize that SEMA7A mediated tumor cell production of FN activates integrin
283 mediated PI3K signaling leading to activation of AKT and cell survival [26, 43]. We also
284 show that SEMA7A promotes mesenchymal phenotypes and tumor cell invasion, which
285 could may be mediated by FN engagement of $\alpha_v\beta_1$-integrin and downstream activation
286 of Slug resulting in transcription of mesenchymal genes [44, 45]. In support of this
287 hypothesis, SEMA7A is linked to EMT in a murine model of BC where TGFβ fails to
288 induce EMT in the absence of SEMA7A [17]. Additional studies to determine how
289 SEMA7A and FN contribute to EMT in our model are necessary to fully understand this
290 mechanism in BC progression.
291 Since upregulation of EMT pathways such as Snail, Slug, and Zeb1 are
292 associated with decreased sensitivity to chemotherapeutic drugs and targeted tyrosine
293 kinase inhibitors (TKIs) [17, 46-55], it is also possible that SEMA7A may promote

294 metastasis by conferring resistance to current therapies. In support of this, SEMA7A
295 promotes resistance to EGFR targeted therapies in lung cancer [13]. Additional studies
296 will explore the role of SEMA7A in resistance and/or susceptibility to current therapies in
297 BC. Moreover, one major limitation of our current study is investigation of this
298 mechanism only in ER- models, which is supported, in part, by our patient dataset
299 studies showing that SEMA7A expression invokes a higher risk for metastasis in ER-
300 breast cancers compared to all breast cancer. However, since ER+ breast cancers
301 comprise the largest percentage of breast cancers in women, additional studies in ER+
302 breast cancers must be performed. Interestingly, estrogen and/or progesterone promote
303 SEMA7A expression in the hypothalamus, suggesting that hormones may drive
304 elevated levels of SEMA7A in BCs [56]. Furthermore, in hormone-receptor positive
305 (HR+) BCs both AKT and FN promote tamoxifen resistance [57-64] and Semaphorin
306 4C, which is structurally similar to SEMA7A, drives hormonal-independence in HR+ BCs
307 [65]. Thus, we are also exploring the relationship between SEMA7A expression and
308 tumor progression in ER+ models [66].

309 We also demonstrate that SEMA7A is also involved in a non-cell-autonomous
310 signaling axis via induction of fibroblast production of collagen, which then promotes
311 COX-2 expression in the tumor cell [4]. Collagen has been characterized for multiple
312 roles in promoting tumor progression as well as increased breast density, which can
313 also increase risk for developing BC [8, 67, 68]. Additionally, a single pregnancy is
314 sufficient to convert the high collagen content of the postpartum breast into pro-
315 tumorigenic collagen [69] and activated fibroblasts, which deposit collagen, are present
316 during postpartum involution [4, 8, 23]. Thus, our previous studies showing that

317 SEMA7A is expressed in the postpartum mammary epithelium during involution
318 SEMA7A, coupled with those presented herein, suggest that SEMA7A could also play a
319 role in the increased risk for developing BC after pregnancy via increasing collagen
320 deposition [1, 4, 31, 67, 68]. COX-2 is also well characterized for multiple roles in tumor
321 initiation and progression [70, 71]. While our results suggest that SEMA7A stimulates
322 collagen production by fibroblasts to result in tumor cell expression of COX-2 we still do
323 not fully understand this mechanism. Additionally, our current studies have not
324 addressed whether COX-2 activity is increased in tumor cells on collagen. Our data also
325 suggest SEMA7A activation of AKT may play a role in promoting survival via
326 upregulation of COX-2. Further studies are needed to understand the molecular
327 mechanisms underlying SEMA7A and COX-2 signaling, regulation, and their roles in
328 promoting tumor cell invasion and survival.
329 Currently there are no prevention strategies, targeted therapies, or specific
330 treatment options for women diagnosed postpartum or for women with high tumor
331 expression of SEMA7A. If our proposed SEMA7A mediated mechanism of progression
332 is also dependent on COX-2 activity, as is suggested by our previous studies [4, 7], the
333 addition of a COX-2 inhibitor to current treatment regimens could have efficacy in
334 postpartum or SEMA7A+ BC patients. We also propose that SEMA7A expression could
335 predict progression or itself be a potential therapeutic target for BC patients. If direct
336 targeting of SEMA7A is not feasible, SEMA7A activates downstream targets such as
337 FAK, Src, and ERK [16, 72], for which targeted therapies are available. Although these
338 targeted inhibitors have been largely unsuccessful in BC, SEMA7A could serve as a
339 predictive biomarker for patients who may benefit. Since metastases are the leading

340 cause of BC related deaths and are largely untreatable, these novel anti-metastatic
341 treatment strategies should be explored.
342
343 **MATERIALS AND METHODS**

344 **Cell Culture**

345 MCF10DCIS and MDA-MB-231 were cultured in 2D and 3D cultures as previously
346 described [4, 18, 22]. MCF10DCIS cells and previously described shCOX-2 derivatives
347 [73] were obtained from K. Polyak and A. Marusyk (Harvard University, Cambridge,
348 MA). MDA-MB-231 cells were obtained from P. Schedin (Oregon Heath and Sciences
349 University, Portland OR). HLF-1 cells were gifted from M. Fini (CU Anschutz Medical
350 Campus, Denver, CO). Cells were validated by the DNA sequencing core at the CU
351 Anschutz Medical Campus and identified to be a pure population of their respective cell
352 lines. Cells were regularly tested for mycoplasma throughout studies. shRNA silencing
353 was achieved using shRNA SEMA7A targeting plasmids (SABiosciences, Frederik, MD,
354 and Functional Genomics Facility at CU Anschutz Medical Campus, Denver, CO) and
355 confirmed via qPCR and Western blot analysis. Overexpression plasmid (SEMA7A-Fc)
356 was a generous gift from R. Medzhitov (Yale University, New Haven, CT). Control
357 plasmid (pcDNA3.1) was obtained from H. Ford (CU Anschutz Medical Campus,
358 Denver, CO). All other overexpression plasmids (p304-V5-Blasticidin and V5-SEMA7A)
359 were obtained from the Functional Genomics Core at the CU Anschutz Medical Campus
360 and overexpression was confirmed via qPCR and Western blot analysis. Purified
361 SEMA7A was isolated from MDA-MB-231 cells engineered to overexpress SEMA7A-Fc
362 in collaboration with the Protein Purification/MoAB/Tissue culture core at the CU
363 Anschutz Medical Campus. Cells were forced into suspension by coating plates with 12

364 mg/ml poly-HEMA (poly (2-hydroxyethyl methacrylate), Sigma, St. Louis, MO) prior to
365 plating.

366 **Tissue microarray**

367 Tissue microarrays containing normal and DCIS samples were prepared from biopsy
368 tissue following placement in preservation media (LiforCell, Lifeblood Medical, Inc.) and
369 storage at 4ºC, as previously described [74].

370 **qPCR**

371 RNA was isolated and qPCR were performed as previously described, with GAPDH and
372 RPS18 as reference genes [18]. Primers for SEMA7A, COL1A1, COX-2 were obtained
373 from Bio-Rad (Bio-Rad PrimePCR, Hercules, CA). Other primers were designed to be
374 intron spanning with the following sequences: GAPDH (forward:
375 CAAGAGCACAAGAGGAA GAGAG, reverse: CTACATGGCAACTGTGAGGAG) and
376 RPS18 (forward: GCGAGTACTCAACACCAACA, reverse:
377 GCTAGGACCTGGCTGTATTT).

378 **Immunoblot analysis**

379 Western blots were performed as previously described [18]. Antibody information is
380 provided in STable2.

381 **Animal model**

382 The MCF10DCIS model was utilized as previously described [4, 18]. Briefly, 6-8-week-
383 old female SCID Hairless Outbread mice from Charles River were bred and, after birth,
384 pup numbers were normalized to 6-8 pups per dam. After 10-13 days of lactation, pups
385 were removed to initiate involution (Day 0). Subsequently, injections of 250K
386 MCF10DCIS controls and cells with shSEMA7A were initiated one day post-weaning

387 (involution day 1) bilaterally into the #4 mammary fat pads. For SEMA7A
388 overexpressing studies, 6-8-week-old Nude athymic (nulliparous) from Charles River
389 were utilized because they are more cost-effective than SCID mice and breeding is not
390 necessary for studies in nulliparous hosts. Tumors were measured twice weekly. For
391 metastasis studies, nude mice were injected with $1x10^6$ cells into the tail vein, monitored
392 for weight loss and sacrificed 3 weeks post-injection.

393 **Histologic analysis**

394 Mammary glands with intact tumor were prepared for immunohistochemistry as
395 previously described [4, 7]. Hematoxylin and eosin stained sections were examined by a
396 board-certified anatomic pathologist (ACN) as scored as follows: 0-lesions which
397 contained only well-devolved DCIS structures with clearly defined basement
398 membranes and no evidence of microinvasion; 1-lesions that contained extensive DCIS
399 with identifiable micro-invasive foci; 2-lesions that contained significant areas of sheet-
400 like invasive tumor growth and mixed with areas of DCIS; 3-lesions that contained
401 entirely invasive tumor with rare to absent DCIS remnants. The pathologist was blinded
402 to study group by the randomization of animal numbers in each group.

403 **Immunohistochemistry and Immunofluorescence**

404 For FN and COX-2 400X images were taken of intact tumor and quantitated using
405 ImageJ software. For SEMA7A, cleaved caspase-3, and trichrome, stain quantification
406 of total tumor area (necrotic and stromal areas removed) and percent positive stain or
407 stain intensity was performed using ImageScope Aperio Analysis software (Leica,
408 Buffalo Grove, IL). Areas for quantification were annotated using Aperio analysis tools
409 and percent weak, medium, and strong determined using the color-deconvolution

410 algorithm. For COX-2 and FN analysis, areas for quantification were isolated from the
411 surrounding stroma and percent positive calculated as area with positive stain (positive
412 pixels) using Image J and divided by total area (total pixels) and multiplied by
413 100.Immunofluorescent images were obtained using 400X magnification on OLYMPUS
414 microscope. Antibody information is provided in STable 2.

415 **In vitro cell death assay**

416 Cell death was analyzed using Caspase-Glo 3/7 Assay (Promega, Madison, WI),
417 according to the manufacturer's instructions.

418 **Analysis of publicly available datasets**

419 Km plotter was queried for BC, and SEMA7A, PTGS2 (COX-2), and FN1 using the
420 multigene classifier mean centered option for distant metastasis free survival (DMFS)
421 [75]. ER- status was determined from ESR1 gene expression data. Ma breast cancer
422 dataset was queried for SEMA7A, PTGS2 (COX-2), and FN1 using Gene expression-
423 based Outcome for Breast Cancer Online (GOBO). TCGA was queried for co-
424 expression of SEMA7A and COX-2 or FN1 using CBioPortal.

425 **Mass spectrometry analysis**

426 Small tumor sections (~1mm) were placed on gelatin sponges (Novartis Animal Heath,
427 Greensboro, NC, USA) in serum-free media as previously described [76]. After 48
428 hours, tumor conditioned media was collected ~ 30 µg of total protein digested utilizing
429 the filter-aided sample digestion (FASP) protocol as previously described according to
430 MAIPE standards [77]. Briefly, samples were reduced, alkylated, and enzymatically
431 digested with trypsin. Resulting peptides were concentrated and de-salted by solid
432 phase extraction utilizing in-house made stage tips made with Sytrene Divinyl Benzene

433 disks (Empore™). Liquid chromatography tandem mass spectrometry (LC-MS/MS) was
434 performed on a Thermo nanoEasy LC II coupled to a Q Exactive HF. MS acquisition
435 parameters are detailed previously [78]. Raw files were searched with Proteome
436 Discoverer 2.2 against the Mus Musculus, Homo Sapiens, and Bos Taurus uniprotKB
437 database in Mascot. Precursor mass tolerance was set to +/- 10 ppm and MS/MS
438 fragment ion tolerance of +/- 25 ppm. Trypsin specificity was selected allowing for 1
439 missed cleavage. Variable modifications include Met oxidation, proline hydroxylation,
440 protein N-terminal acetylation, peptide N-terminal pyroglutamic acid formation, and a
441 fixed modification of Cys carbamidomethylation.
442 Search results were visualized using Metaboanalyst v4.0 [79] and gene ontology
443 mapping was done using PANTHER [80]. Data were prepared according to MIAPE
444 standards and will be made available upon publication.
445 **Experimental replicates, sample size and statistical analyses.**
446 All in vitro studies were performed in biological triplicates. For animal studies, we chose
447 the number of mice/group/time-point, based on power calculations form previous and
448 pilot studies to achieve at least 80% power (β) with α=0.05. All animal studies were
449 replicated twice with representative or pooled data shown. Unpaired and paired t-tests,
450 ANOVA, and Kaplan Meier statistical analyses were performed in GraphPad Prism,
451 assuming independent samples and normal distributions. Analyses for Figure 2 were
452 done using one-tailed t-tests, as our results from Figure 1 would predict significant
453 differences between groups. All other analyses were done using two-tailed tests. Only
454 p-values of less than 0.05 were considered significant. Aside from unexpended death or
455 cell contamination, no samples or animals were excluded from our analysis. For IHC

456 analysis of tumors, outliers were removed if they were significant by the ROUT (Q=1%)
457 test.

458 **Study Approval**

459 Prior to resection, patients provided written informed consent under an IRB-approved
460 protocol according to the guidelines of their respective institutions and conducted in
461 compliance with HIPPA regulations. All animal studies were approved by the IACUC of
462 the CU Anschutz Medical Campus, protocol number B106017(06)1E.

463

464 **Author Contributions**

465 SET and TRL conceived and designed the study. SET performed all in vitro and in vivo
466 studies. VFB and FB were responsible for regulatory oversight of human tissue
467 acquisition and providing cases for IHC analysis. RCH and KH were responsible for all
468 mass spectrometry experiments and associated data analysis. ACN was responsible for
469 analyzing and scoring all tumor for invasion. SET and TRL were responsible for
470 hypothesis development, conceptual design, data analysis and data interpretation. SET
471 and TRL wrote the manuscript with all authors providing critical evaluation.

472 **Acknowledgements**

473 MCF10DCIS cells were obtained from K. Polyak and A. Marusyk (Harvard University,
474 Cambridge, MA). MDA-MB-231 cells were obtained from P. Schedin (Oregon Heath and
475 Sciences University, Portland OR). HLF-1 cells were gifted from M. Fini (CU Anschutz
476 Medical Campus, Denver, CO). H. Ford for the pcDNA3.1 vector (CU Anschutz Medical
477 Campus, Denver, CO).; and R. Medzhitov (Yale University, New Haven, CT) for the
478 SEMA7A-Fc overexpression vector. We also acknowledge V. Wessells, A. Elder, L.
479 Crump, T. Wallace, C. Young, A. Stoller, M. Kobritz, and C. Hoang for technical support
480 and advice. This work was supported by the American Cancer Society (RSG 16-171-01-
481 CSM), and NIH/NCI (R01CA211696-01A1) to T. Lyons; NIH/CCTSI/CTSA (TL1
482 TR001081) to S. Tarullo.

483

484 **Supplementary Information** is available on *Oncogene's* website.

References

1 Callihan EB, Gao D, Jindal S, Lyons TR, Manthey E, Edgerton S *et al*. Postpartum diagnosis demonstrates a high risk for metastasis and merits an expanded definition of pregnancy-associated breast cancer. *Breast cancer research and treatment* 2013; 138: 549-559.

2 Erica T. Goddard SB, Troy Schedin, Sonali Jindal, Jeremy Johnston, Ethan Cabral, Traci R. Lyons, Motomi Mori, Pepper J. Schedin, Virginia F. Borges. Defining the impact of a postpartum diagnosis on metastasis and the clinical features underlying risk: A young women's breast cancer cohort study. *Jama Network* 2018; In press.

3 Nichols HB, Schoemaker MJ, Cai J, Xu J, Wright LB, Brook MN *et al*. Breast Cancer Risk After Recent Childbirth: A Pooled Analysis of 15 Prospective Studies. *Ann Intern Med* 2018.

4 Lyons TR, O'Brien J, Borges VF, Conklin MW, Keely PJ, Eliceiri KW *et al*. Postpartum mammary gland involution drives progression of ductal carcinoma in situ through collagen and COX-2. *Nature medicine* 2011; 17: 1109-1115.

5 Slepicka PF, Cyrill SL, Dos Santos CO. Pregnancy and Breast Cancer: Pathways to Understand Risk and Prevention. *Trends Mol Med* 2019.

6 Elder AM, Tamburini BAJ, Crump LS, Black SA, Wessells VM, Schedin PJ *et al*. Semaphorin 7A Promotes Macrophage-Mediated Lymphatic Remodeling during Postpartum Mammary Gland Involution and in Breast Cancer. *Cancer research* 2018; 78: 6473-6485.

7 Lyons TR, Borges VF, Betts CB, Guo Q, Kapoor P, Martinson HA *et al*. Cyclooxygenase-2-dependent lymphangiogenesis promotes nodal metastasis of postpartum breast cancer. *The Journal of clinical investigation* 2014; 124: 3901-3912.

8 Guo Q, Minnier J, Burchard J, Chiotti K, Spellman P, Schedin P. Physiologically activated mammary fibroblasts promote postpartum mammary cancer. *JCI Insight* 2017; 2: e89206.

9 Asztalos S, Gann PH, Hayes MK, Nonn L, Beam CA, Dai Y *et al*. Gene expression patterns in the human breast after pregnancy. *Cancer Prev Res (Phila)* 2010; 3: 301-311.

10 Miller FR, Santner SJ, Tait L, Dawson PJ. MCF10DCIS.com xenograft model of human comedo ductal carcinoma in situ. *Journal of the National Cancer Institute* 2000; 92: 1185-1186.

11 Gupta PB, Proia D, Cingoz O, Weremowicz J, Naber SP, Weinberg RA *et al*. Systemic stromal effects of estrogen promote the growth of estrogen receptor-negative cancers. *Cancer research* 2007; 67: 2062-2071.

12 Rehman M, Tamagnone L. Semaphorins in cancer: biological mechanisms and therapeutic approaches. *Semin Cell Dev Biol* 2013; 24: 179-189.

13 Kinehara Y, Nagatomo I, Koyama S, Ito D, Nojima S, Kurebayashi R *et al*. Semaphorin 7A promotes EGFR-TKI resistance in EGFR mutant lung adenocarcinoma cells. *JCI Insight* 2018; 3.

14 Ma B, Herzog EL, Lee CG, Peng X, Lee CM, Chen X *et al*. Role of chitinase 3-like-1 and semaphorin 7a in pulmonary melanoma metastasis. *Cancer research* 2015; 75: 487-496.

15 Saito T, Kasamatsu A, Ogawara K, Miyamoto I, Saito K, Iyoda M *et al*. Semaphorin7A promotion of tumoral growth and metastasis in human oral cancer by regulation of g1 cell cycle and matrix metalloproteases: Possible contribution to tumoral angiogenesis. *PloS one* 2015; 10: 1-20.

16 Scott Ga, McClelland La, Fricke AF, Fender A. Plexin C1, A Receptor for Semaphorin 7A, Inactivates Cofilin and Is a Potential Tumor Suppressor for Melanoma Progression. *Journal of Investigative Dermatology* 2009; 129: 954-963.

17 Allegra M, Zaragkoulias A, Vorgia E, Ioannou M, Litos G, Beug H *et al*. Semaphorin-7a reverses the ERF-induced inhibition of EMT in Ras-dependent mouse mammary epithelial cells. *Molecular biology of the cell* 2012; 23: 3873-3881.

18 Black SA, Nelson AC, Gurule NJ, Futscher BW, Lyons TR. Semaphorin 7a exerts pleiotropic effects to promote breast tumor progression. *Oncogene* 2016; 35: 5170-5178.

19 Garcia-Areas R, Libreros S, Amat S, Keating P, Carrio R, Robinson P *et al*. Semaphorin7A promotes tumor growth and exerts a pro-angiogenic effect in macrophages of mammary tumor-bearing mice. *Frontiers in physiology* 2014; 5: 17.

20 Garcia-Areas R, Libreros S, Simoes M, Castro-Silva C, Gazaniga N, Amat S *et al*. Suppression of tumor-derived Semaphorin 7A and genetic ablation of host-derived Semaphorin 7A impairs tumor progression in a murine model of advanced breast carcinoma. *Int J Oncol* 2017; 51: 1395-1404.

575 21 Curtis C, Shah SP, Chin SF, Turashvili G, Rueda OM, Dunning MJ *et al*. The
576 genomic and transcriptomic architecture of 2,000 breast tumours reveals novel
577 subgroups. *Nature* 2012; 486: 346-352.
578
579 22 Jacob A, Jing J, Lee J, Schedin P, Gilbert SM, Peden AA *et al*. Rab40b regulates
580 trafficking of MMP2 and MMP9 during invadopodia formation and invasion of
581 breast cancer cells. *Journal of cell science* 2013; 126: 4647-4658.
582
583 23 Maller O, Hansen KC, Lyons TR, Acerbi I, Weaver VM, Prekeris R *et al*. Collagen
584 architecture in pregnancy-induced protection from breast cancer. *Journal of cell*
585 *science* 2013; 126: 4108-4110.
586
587 24 Kalluri R, Weinberg RA. The basics of epithelial-mesenchymal transition. *The*
588 *Journal of clinical investigation* 2009; 119: 1420-1428.
589
590 25 Balmanno K, Cook SJ. Tumour cell survival signalling by the ERK1/2 pathway.
591 *Cell death and differentiation* (Review) 2008; 16: 368.
592
593 26 Reddig PJ, Juliano RL. Clinging to life: cell to matrix adhesion and cell survival.
594 *Cancer Metastasis Rev* 2005; 24: 425-439.
595
596 27 Tiwari N, Gheldof A, Tatari M, Christofori G. EMT as the ultimate survival
597 mechanism of cancer cells. *Seminars in Cancer Biology* 2012; 22: 194-207.
598
599 28 St-Germain ME, Gagnon V, Parent S, Asselin E. Regulation of COX-2 protein
600 expression by Akt in endometrial cancer cells is mediated through NF-
601 kappaB/IkappaB pathway. *Mol Cancer* 2004; 3: 7.
602
603 29 Schedin P. Pregnancy-associated breast cancer and metastasis. *Nature reviews*
604 *Cancer* 2006; 6: 281-291.
605
606 30 Albrektsen G, Heuch I, Hansen S, Kvale G. Breast cancer risk by age at birth,
607 time since birth and time intervals between births: exploring interaction effects.
608 *British journal of cancer* 2005; 92: 167-175.
609
610 31 Goddard ET, Bassale S, Schedin T, Jindal S, Johnston J, Cabral E *et al*.
611 Association Between Postpartum Breast Cancer Diagnosis and Metastasis and
612 the Clinical Features Underlying Risk. *JAMA Netw Open* 2019; 2: e186997.
613
614 32 Welch DRA-Ohoo, Hurst DRA-Ohoo. Defining the Hallmarks of Metastasis. LID -
615 10.1158/0008-5472.CAN-19-0458 [doi].
616
617 33 Cerny J, Stockinger H, Horejsi V. Noncovalent associations of T lymphocyte
618 surface proteins. *Eur J Immunol* 1996; 26: 2335-2343.
619

620 34 Zhou Y, Gunput RA, Pasterkamp RJ. Semaphorin signaling: progress made and
621 promises ahead. *Trends in biochemical sciences* 2008; 33: 161-170.
622
623 35 Liu H, Juo ZS, Shim AH, Focia PJ, Chen X, Garcia KC *et al*. Structural basis of
624 semaphorin-plexin recognition and viral mimicry from Sema7A and A39R
625 complexes with PlexinC1. *Cell* 2010; 142: 749-761.
626
627 36 Fong KP, Barry C, Tran AN, Traxler Ea, Wannemacher KM, Tang HY *et al*.
628 Deciphering the human platelet sheddome. *Blood* 2011; 117: 15-27.
629
630 37 Jaimes Y, Gras C, Goudeva L, Buchholz S, Eiz-Vesper B, Seltsam A *et al*.
631 Semaphorin 7A inhibits platelet production from CD34+ progenitor cells. *Journal*
632 *of thrombosis and haemostasis : JTH* 2012; 10: 1100-1108.
633
634 38 Xie J, Wang H. Semaphorin 7A as a potential immune regulator and promising
635 therapeutic target in rheumatoid arthritis. *Arthritis Res Ther* 2017; 19: 10.
636
637 39 Kopp MA, Brommer B, Gatzemeier N, Schwab JM, Pruss H. Spinal cord injury
638 induces differential expression of the profibrotic semaphorin 7A in the developing
639 and mature glial scar. *Glia* 2010; 58: 1748-1756.
640
641 40 Gan Y, Reilkoff R, Peng X, Russell T, Chen Q, Mathai SK *et al*. Role of
642 semaphorin 7a signaling in transforming growth factor beta1-induced lung
643 fibrosis and scleroderma-related interstitial lung disease. *Arthritis and*
644 *rheumatism* 2011; 63: 2484-2494.
645
646 41 Reilkoff RA, Peng H, Murray LA, Peng X, Russell T, Montgomery R *et al*.
647 Semaphorin 7a+ regulatory T cells are associated with progressive idiopathic
648 pulmonary fibrosis and are implicated in transforming growth factor-beta1-
649 induced pulmonary fibrosis. *American journal of respiratory and critical care*
650 *medicine* 2013; 187: 180-188.
651
652 42 Kang H-R, Lee CG, Homer RJ, Elias Ja. Semaphorin 7A plays a critical role in
653 TGF-beta1-induced pulmonary fibrosis. *The Journal of experimental medicine*
654 2007; 204: 1083-1093.
655
656 43 Gilmore AP, Owens TW, Foster FM, Lindsay J. How adhesion signals reach a
657 mitochondrial conclusion--ECM regulation of apoptosis. *Current opinion in cell*
658 *biology* 2009; 21: 654-661.
659
660 44 Knowles LM, Gurski LA, Engel C, Gnarra JR, Maranchie JK, Pilch J. Integrin
661 αvβ3 and fibronectin upregulate Slug in cancer cells to promote clot invasion and
662 metastasis. *Cancer research* 2013; 73: 6175-6184.
663
664 45 Lamouille S, Xu J, Derynck R. Molecular mechanisms of epithelial-mesenchymal
665 transition. *Nature reviews Molecular cell biology* 2014; 15: 178-196.

46 Chao Y, Wu Q, Acquafondata M, Dhir R, Wells A. Partial mesenchymal to epithelial reverting transition in breast and prostate cancer metastases. *Cancer microenvironment : official journal of the International Cancer Microenvironment Society* 2012; 5: 19-28.

47 Smith BN, Bhowmick NA. Role of EMT in Metastasis and Therapy Resistance. *J Clin Med* 2016; 5.

48 Nurwidya F, Murakami A, Takahashi F, Takahashi K. Molecular mechanisms contributing to resistance to tyrosine kinase-targeted therapy for non-small cell lung cancer. *Cancer biology & medicine* 2012; 9: 18-22.

49 Nurwidya F, Takahashi F, Murakami A, Takahashi K. Epithelial mesenchymal transition in drug resistance and metastasis of lung cancer. *Cancer research and treatment : official journal of Korean Cancer Association* 2012; 44: 151-156.

50 Uchikado Y, Okumura H, Ishigami S, Setoyama T, Matsumoto M, Owaki T *et al*. Increased Slug and decreased E-cadherin expression is related to poor prognosis in patients with gastric cancer. *Gastric cancer : official journal of the International Gastric Cancer Association and the Japanese Gastric Cancer Association* 2011; 14: 41-49.

51 Deep G, Jain AK, Ramteke A, Ting H, Vijendra KC, Gangar SC *et al*. SNAI1 is critical for the aggressiveness of prostate cancer cells with low E-cadherin. *Mol Cancer* 2014; 13: 37.

52 McKeithen D, Graham T, Chung LW, Odero-Marah V. Snail transcription factor regulates neuroendocrine differentiation in LNCaP prostate cancer cells. *Prostate* 2010; 70: 982-992.

53 Cheng GZ, Chan J, Wang Q, Zhang W, Sun CD, Wang LH. Twist transcriptionally up-regulates AKT2 in breast cancer cells leading to increased migration, invasion, and resistance to paclitaxel. *Cancer research* 2007; 67: 1979-1987.

54 Baritaki S, Yeung K, Palladino M, Berenson J, Bonavida B. Pivotal roles of snail inhibition and RKIP induction by the proteasome inhibitor NPI-0052 in tumor cell chemoimmunosensitization. *Cancer research* 2009; 69: 8376-8385.

55 Vesuna F, Lisok A, Kimble B, Domek J, Kato Y, van der Groep P *et al*. Twist contributes to hormone resistance in breast cancer by downregulating estrogen receptor-alpha. *Oncogene* 2012; 31: 3223-3234.

710 56 Parkash J, Messina A, Langlet F, Cimino I, Loyens A, Mazur D *et al*.
711 Semaphorin7A regulates neuroglial plasticity in the adult hypothalamic median
712 eminence. *Nature communications* 2015; 6: 6385.
713
714 57 Eke I, Storch K, Krause M, Cordes N. Cetuximab attenuates its cytotoxic and
715 radiosensitizing potential by inducing fibronectin biosynthesis. *Cancer research*
716 2013; 73: 5869-5879.
717
718 58 Pontiggia O, Sampayo R, Raffo D, Motter A, Xu R, Bissell MJ *et al*. The tumor
719 microenvironment modulates tamoxifen resistance in breast cancer: a role for
720 soluble stromal factors and fibronectin through beta1 integrin. *Breast cancer*
721 *research and treatment* 2012; 133: 459-471.
722
723 59 Han SW, Roman J. Fibronectin induces cell proliferation and inhibits apoptosis in
724 human bronchial epithelial cells: pro-oncogenic effects mediated by PI3-kinase
725 and NF-kappa B. *Oncogene* 2006; 25: 4341-4349.
726
727 60 Hattar R, Maller O, McDaniel S, Hansen KC, Hedman KJ, Lyons TR *et al*.
728 Tamoxifen induces pleiotrophic changes in mammary stroma resulting in
729 extracellular matrix that suppresses transformed phenotypes. *Breast cancer*
730 *research : BCR* 2009; 11: R5.
731
732 61 Cheng JQ, Jiang X, Fraser M, Li M, Dan HC, Sun M *et al*. Role of X-linked
733 inhibitor of apoptosis protein in chemoresistance in ovarian cancer: possible
734 involvement of the phosphoinositide-3 kinase/Akt pathway. *Drug resistance*
735 *updates : reviews and commentaries in antimicrobial and anticancer*
736 *chemotherapy* 2002; 5: 131-146.
737
738 62 Fraser M, Leung BM, Yan X, Dan HC, Cheng JQ, Tsang BK. p53 is a
739 determinant of X-linked inhibitor of apoptosis protein/Akt-mediated
740 chemoresistance in human ovarian cancer cells. *Cancer research* 2003; 63:
741 7081-7088.
742
743 63 Knuefermann C, Lu Y, Liu B, Jin W, Liang K, Wu L *et al*. HER2/PI-3K/Akt
744 activation leads to a multidrug resistance in human breast adenocarcinoma cells.
745 *Oncogene* 2003; 22: 3205-3212.
746
747 64 Li J, Feng Q, Kim JM, Schneiderman D, Liston P, Li M *et al*. Human ovarian
748 cancer and cisplatin resistance: possible role of inhibitor of apoptosis proteins.
749 *Endocrinology* 2001; 142: 370-380.
750
751 65 Gurrapu S, Pupo E, Franzolin G, Lanzetti L, Tamagnone LA-Ohoo.
752 Sema4C/PlexinB2 signaling controls breast cancer cell growth, hormonal
753 dependence and tumorigenic potential.
754

66 Crump LS, Wyatt G, Porter WW, Richer J, Lyons TR. Hormonal regulation of Semaphorin 7a in ER+ breast cancer drives therapeutic resistance. *bioRxiv* 2019: 650135.

67 Provenzano PP, Eliceiri KW, Campbell JM, Inman DR, White JG, Keely PJ. Collagen reorganization at the tumor-stromal interface facilitates local invasion. *BMC medicine* 2006; 4: 38.

68 Provenzano PP, Inman DR, Eliceiri KW, Knittel JG, Yan L, Rueden CT *et al*. Collagen density promotes mammary tumor initiation and progression. *BMC medicine* 2008; 6: 11-11.

69 Slocum E, Craig A, Villanueva A, Germain D. Parity predisposes breasts to the oncogenic action of PAPP-A and activation of the collagen receptor DDR2.

70 Ristimäki A, Sivula A, Lundin J, Ristima A, Lundin M, Salminen T *et al*. Prognostic Significance of Elevated Cyclooxygenase-2 Expression in Breast Cancer Advances in Brief Prognostic Significance of Elevated Cyclooxygenase-2 Expression in Breast Cancer 12002: 632-635.

71 Denkert C, Winzer K-J, Müller B-M, Weichert W, Pest S, Köbel M *et al*. Elevated expression of cyclooxygenase-2 is a negative prognostic factor for disease free survival and overall survival in patients with breast carcinoma. *Cancer* 2003; 97: 2978-2987.

72 Pasterkamp RJ, Peschon JJ, Spriggs MK, Kolodkin AL. Semaphorin 7A promotes axon outgrowth through integrins and MAPKs. *Nature* 2003; 424: 398-405.

73 Hu M, Peluffo G, Chen H, Gelman R, Schnitt S, Polyak K. Role of COX-2 in epithelial-stromal cell interactions and progression of ductal carcinoma in situ of the breast. *Proceedings of the National Academy of Sciences of the United States of America* 2009; 106: 3372-3377.

74 Valdez KE, Fan F Fau - Smith W, Smith W Fau - Allred DC, Allred Dc Fau - Medina D, Medina D Fau - Behbod F, Behbod F. Human primary ductal carcinoma in situ (DCIS) subtype-specific pathology is preserved in a mouse intraductal (MIND) xenograft model.

75 Nagy A, Lanczky A, Menyhart O, Gyorffy B. Author Correction: Validation of miRNA prognostic power in hepatocellular carcinoma using expression data of independent datasets. *Scientific reports* 2018; 8: 11515.

76 Dean JL, McClendon aK, Hickey TE, Butler LM, Tilley WD, Witkiewicz AK *et al*. Therapeutic response to CDK4/6 inhibition in breast cancer defined by ex vivo analyses of human tumors. *Cell cycle* 2012; 11: 2756-2761.

77 Barrett AS, Wither MJ, Hill RC, Dzieciatkowska M, D'Alessandro A, Reisz JA *et al*. Hydroxylamine Chemical Digestion for Insoluble Extracellular Matrix Characterization. *Journal of proteome research* 2017; 16: 4177-4184.

78 Reisz JA, Nemkov T, Dzieciatkowska M, Culp-Hill R, Stefanoni D, Hill RC *et al*. Methylation of protein aspartates and deamidated asparagines as a function of blood bank storage and oxidative stress in human red blood cells. *Transfusion* 2018; 58: 2978-2991.

79 Chong J, Xia J. MetaboAnalystR: an R package for flexible and reproducible analysis of metabolomics data. *Bioinformatics* 2018; 34: 4313-4314.

80 Mi H, Muruganujan A, Ebert D, Huang X, Thomas PD. PANTHER version 14: more genomes, a new PANTHER GO-slim and improvements in enrichment analysis tools. *Nucleic acids research* 2019; 47: D419-d426.

820 **<u>Figure 1.</u> SEMA7A promotes growth and invasion in PPBC**. **A.** Tumor volumes for
821 control (Ctrl) or shSEMA7A (SEMA7A-KD) MCF10DCIS cells in postpartum hosts
822 (n=12/group), inset: representative immunoblot for SEMA7A and GAPDH. **B.** Tumors
823 from Ctrl and SEMA7A-KD from postpartum hosts scored for invasion (n=12/group). **C**.
824 Trichrome stained quantification (top) and representative images (bottom) of collagen of
825 tumors from Ctrl and SEMA7A-KD tumors from postpartum hosts, scale bars 50μm
826 (n=12/group) . **D.** IHC quantification (top) and representative images (bottom) of IHC for
827 COX-2 of tumors from Ctrl and SEMA7A-KD tumors from postpartum hosts, scale bars
828 50μm (n=12/group) (*p<0.05, **p<0.01, ***p<0.0005, ****p<0.0001, t-test).
829 **<u>Figure 2.</u> SEMA7A expression is increased in DCIS patient samples. A.**
830 Representative images of normal (top) or DCIS lesions (bottom) from postpartum
831 patients from the CU Anschutz Medical Campus Young Women's BC (YWBC) stained
832 by IHC for SEMA7A, with quantification mask to the right, blue=negative; yellow=weak;
833 orange=medium; red=strong; scale bars 50 μm. **B.** Quantification of SEMA7A IHC of
834 normal or DCIS patient samples from the CU Anschutz YWBC cohort (n=103), then
835 separated by parity status, nulliparous (n=52) or postpartum (n=51). **C**. Quantification of
836 SEMA7A IHC from nulliparous patients by patient, paired t-test. **D.** Quantification of
837 SEMA7A IHC from postpartum patients by patient, paired t-test. **E.** Representative
838 images of SEMA7A IHC stain from tissue array of samples, scale bars 50μm. **F.**
839 Quantification of SEMA7A IHC stain from **C**; normal (n=32) or DCIS (n=30). **G.**
840 Quantification of SEMA7A IHC by patient, paired t-test. (*p<0.05, **p<0.01, ****p<0.001)
841

842 **<u>Figure 3</u>. SEMA7A expression is sufficient to drive tumor growth and invasion**. **A**.
843 Tumor volumes for control (NUL Ctrl) or SEMA7A overexpressing (NUL SEMA7A OE)
844 in nulliparous hosts (n=10/group), inset: representative immunoblot for SEMA7A and
845 GAPDH. **B**. Tumors from NUL Ctrl and NUL SEMA7A OE scored for invasion
846 (n=10/group). **C**. Trichrome stained quantification (top) and representative images
847 (bottom) of collagen of tumors from NUL Ctrl and NUL SEMA7A OE tumors, scale bars
848 50μm **D.** IHC quantification (top) and representative images (bottom) of IHC for COX-2
849 of tumors from NUL Ctrl and NUL SEMA7A OE tumors, scale bars 50μm (*p<0.05,
850 **p<0.01, ***p<0.0005, ****p<0.0001, t-test).
851 **<u>Figure 4</u>. SEMA7A promotes invasion via fibroblast mediated collagen deposition.**
852 **A.** Ctrl or SEMA7A OE MCF10DCIS cells embedded in matrigel scored for invasion. **B.**
853 Ctrl or SEMA7A OE MCF10DCIS cells embedded in matrigel plus 20% collagen. **C**.
854 Control (Ctrl) or shSEMA7A (KD) MDA-MB-231 cells in matrigel plus 25% collagen
855 scored for invasion. **D**. Quantitative RT-PCR (q-PCR) for COL1A1 in fibroblasts in
856 serum free media (SFM) treated with 10 ng/mL TGFβ or conditioned media (CM) from
857 control (Ctrl) or SEMA7A overexpressing (SEMA7A OE) MDA-MB-231 cell lines. **E**.
858 qPCR for COLA1A in fibroblasts in SFM treated with 75 ng/μL purified SEMA7A.
859 (*p<0.05, **p<0.01,***p<0.005, t-test).
860 **<u>Figure 5</u>. SEMA7A promotes mesenchymal protein expression and phenotypes**.
861 **A**. Global proteomics analysis of secreted proteins reveals decreased fibronectin (FN) in
862 MCF10DCIS shSEMA7A (SEMA7A-KD) tumors compared to control (Ctrl) ex vivo
863 (n=10-11/group). **B&C**. IHC for FN in MCF10DCIS Ctrl and SEMA7A-KD tumors (B),
864 and MCF10DCIS Ctrl and SEMA7A overexpressing (SEMA7A OE) tumors, scale bar

865 50μm. **D-F**. Additional decreases in mesenchymal or mesenchymal associated proteins
866 observed by proteomics in shSEMA7A (SEMA7A-KD) tumors ex vivo. **G**.
867 Immunofluorescence for F-actin in MDA-MB-231 Ctrl or KD cells and quantification for
868 cell aspect ratio (length/width). **H**. Immunofluorescence for F-actin in MCF10DCIS Ctrl
869 or SEMA7A OE cells and quantification for cell aspect ratio (length/width). (*p<0.05,
870 **p<0.01, ***p<0.005, ****p<0.001, t-test)
871 **Figure 6. SEMA7A promotes cell survival via fibronectin. A&B**. Fold change of
872 cleaved caspase 3/7 activity in control (Ctrl) and shSEMA7A (KD) in MCF10DCIS (**A**) or
873 MDA-MB-231 (**B**) cell lines. **C.** Cleaved caspase 3/7 activity measured over time in
874 MDA-MB-231 Ctrl or KD cells. **D.** Representative immunoblot for phospho-AKT (S473),
875 total AKT, or GAPDH in Ctrl or KD, quantified to the right. **E**. Cleaved caspase 3/7
876 activity control (Ctrl) or shSEMA7A (KD) cells plated on tissue culture plastic (TC),
877 laminin (LAM), collagen I (COL) or fibronectin (FN). **F&G.** Cleaved caspase 3/7 activity
878 MCF10DCIS (**F**) or MDA-MB-231 (**G**) Ctrl or KD cells in forced suspension. **H.** Cleaved
879 caspase 3/7 activity in MCF10DCIS Ctrl or shCOX-2 (KD1/KD2) cell lines in forced
880 suspension.
881 **Figure 7. SEMA7A drives metastatic seeding and poor prognosis in patients**. **A.**
882 Average area of metastasis in lungs of mice after tail vein injection with MDA-MB-231
883 control (Ctrl) or shSEMA7A (KD1, KD2) cells (n=5/group), representative images of
884 lungs to the right. **B.** Kaplan-Meier analysis of ER- BCs using Km plotter for SEMA7A,
885 COX-2 and FN mRNA expression for distant metastasis free survival (DMFS) (n=228).
886 **C**. Kaplan-Meier analysis of ER-BCs in the Ma Breast Cancer dataset using GOBO for
887 SEMA7A, COX-2 and FN mRNA expression for distant metastasis free survival (DMFS)

888 (n=320) **D&E.** Co-expression analysis of the TCGA BC provisional cohort using

889 CBioPortal for all BCs (n=1108). (*p<0.05, **p<0.01,***p<0.005 ****p<0.001)**.**

890 **Figure 8. Model depicting SEMA7A mediated invasion and cell survival.** Our

891 current data suggests SEMA7A promotes fibroblast mediated collagen deposition,

892 resulting in COX-2 expression and tumor cell invasion. Our results also suggest that

893 SEMA7A can promote cell survival through SEMA7A mediated fibronectin expression.

Figure 1

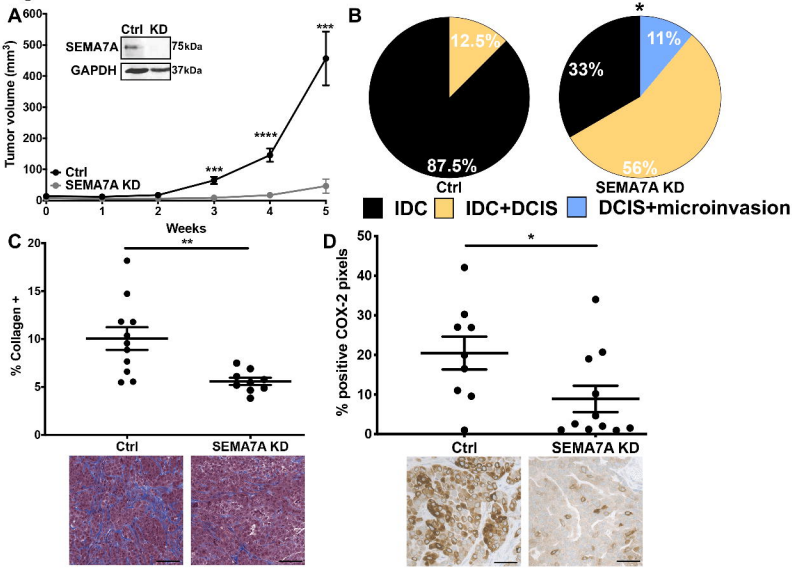
A
Tumor volume (mm³)
Ctrl KD
SEMA7A
75kDa
GAPDH
37kDa
Ctrl
SEMA7A KD
Weeks
***
****
B
12.5%
87.5%
Ctrl
*
11%
33%
56%
SEMA7A KD
IDC
IDC+DCIS
DCIS+microinvasion
C
% Collagen +
**
Ctrl
SEMA7A KD
D
% positive COX-2 pixels
*
Ctrl
SEMA7A KD

Figure 2

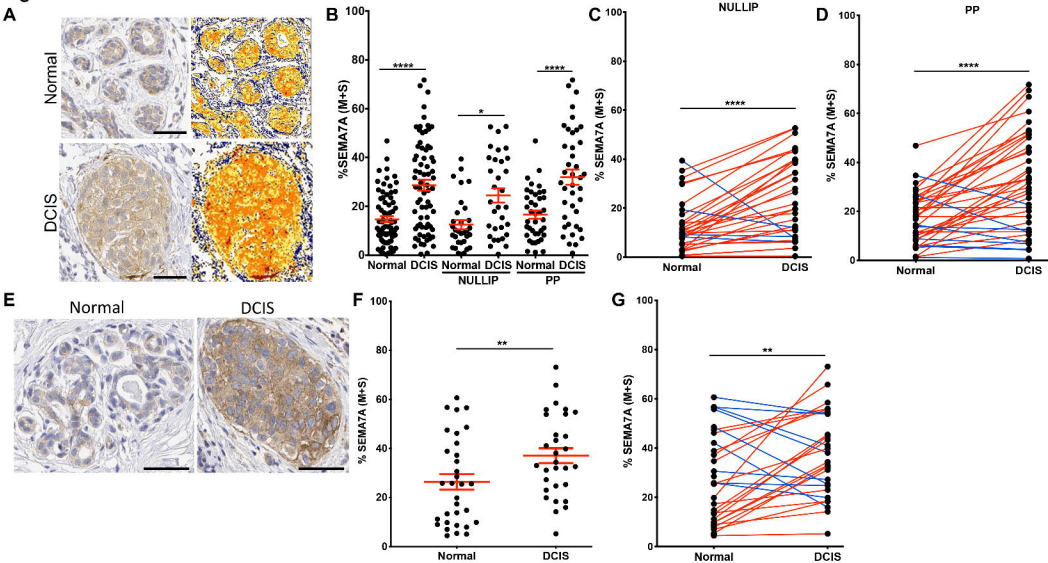
A
Normal
DCIS
B
%SEMA7A (M+S)
****
*
****
Normal
DCIS
Normal
DCIS
Normal
DCIS
NULLIP
PP
C
NULLIP
% SEMA7A (M+S)
****
Normal
DCIS
D
PP
% SEMA7A (M+S)
****
Normal
DCIS
E
Normal
DCIS
F
% SEMA7A (M+S)
**
Normal
DCIS
G
% SEMA7A (M+S)
**
Normal
DCIS

Figure 3

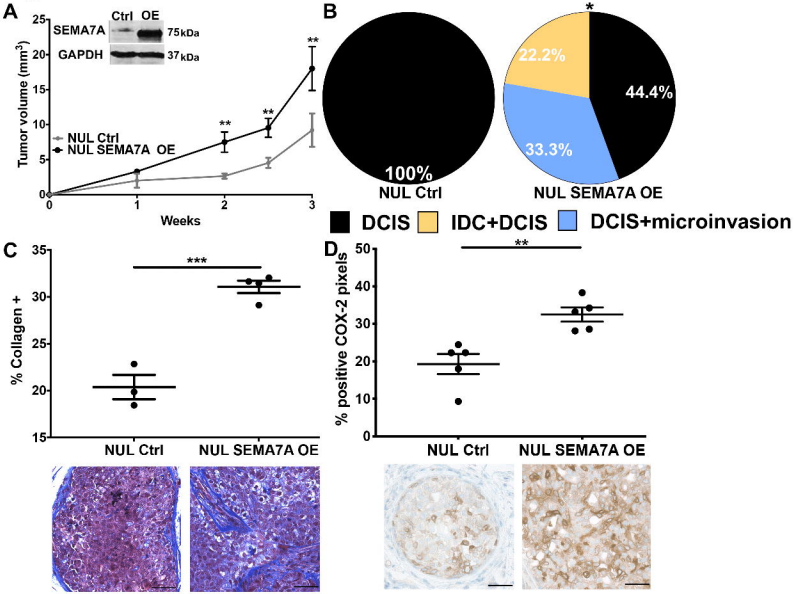
A
Ctrl OE
SEMA7A
GAPDH
75kDa
37kDa
Tumor volume (mm3)
NUL Ctrl
NUL SEMA7A OE
Weeks
B
100%
NUL Ctrl
22.2%
44.4%
33.3%
NUL SEMA7A OE
DCIS
IDC+DCIS
DCIS+microinvasion
C
% Collagen +
NUL Ctrl
NUL SEMA7A OE
D
% positive COX-2 pixels
NUL Ctrl
NUL SEMA7A OE

Figure 4

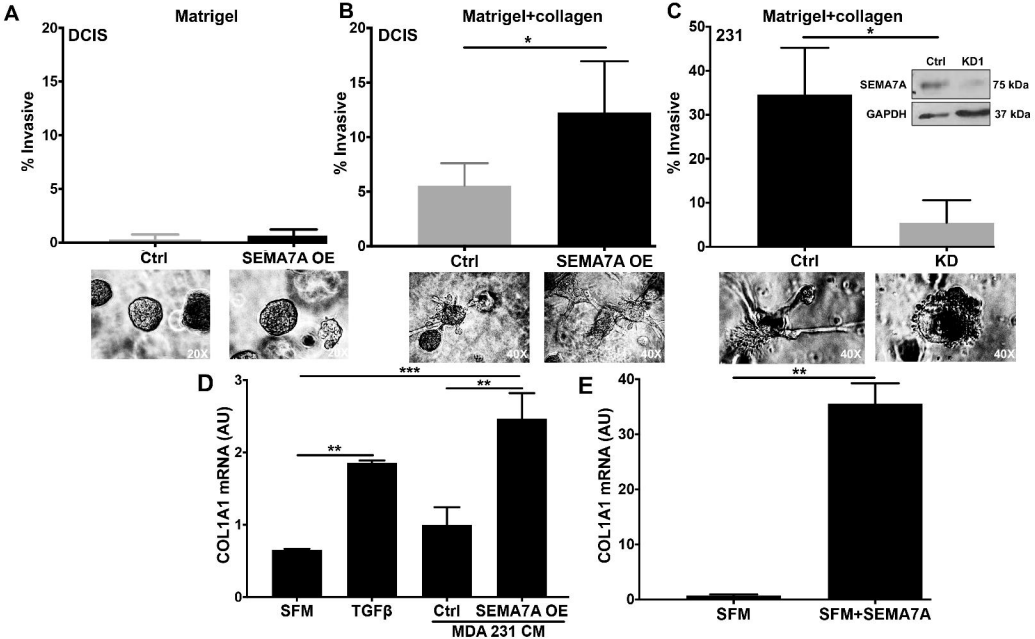
A
Matrigel
DCIS
% Invasive
Ctrl
SEMA7A OE
20X
B
Matrigel+collagen
DCIS
*
% Invasive
Ctrl
SEMA7A OE
40X
40X
C
Matrigel+collagen
231
*
Ctrl
KD1
SEMA7A
75 kDa
GAPDH
37 kDa
% Invasive
Ctrl
KD
40X
40X
D
***
**
**
COL1A1 mRNA (AU)
SFM
TGFβ
Ctrl
SEMA7A OE
MDA 231 CM
E
**
COL1A1 mRNA (AU)
SFM
SFM+SEMA7A

Figure 5

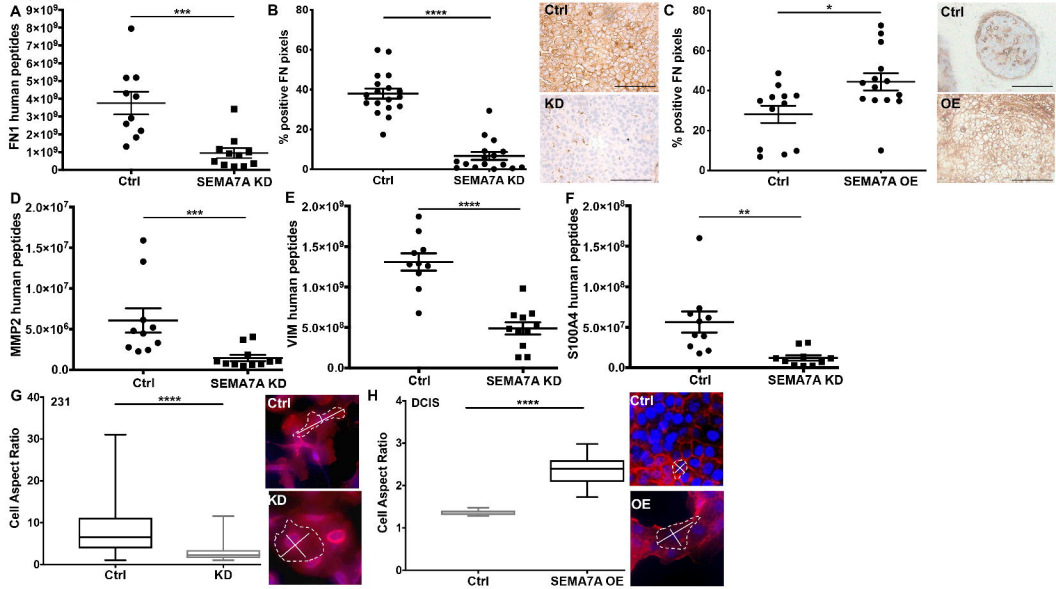
A
FN1 human peptides
9×10⁹
8×10⁹
7×10⁹
6×10⁹
5×10⁹
4×10⁹
3×10⁹
2×10⁹
1×10⁹
0
***
Ctrl
SEMA7A KD
B
% positive FN pixels
80
60
40
20
0
****
Ctrl
SEMA7A KD
Ctrl
KD
C
% positive FN pixels
80
60
40
20
0
*
Ctrl
SEMA7A OE
Ctrl
OE
D
MMP2 human peptides
2.0×10⁷
1.5×10⁷
1.0×10⁷
5.0×10⁶
0.0
***
Ctrl
SEMA7A KD
E
VIM human peptides
2.0×10⁹
1.5×10⁹
1.0×10⁹
5.0×10⁸
0.0
****
Ctrl
SEMA7A KD
F
S100A4 human peptides
2.0×10⁸
1.5×10⁸
1.0×10⁸
5.0×10⁷
0.0
**
Ctrl
SEMA7A KD
G
231
Cell Aspect Ratio
40
30
20
10
0
****
Ctrl
KD
Ctrl
KD
H
DCIS
Cell Aspect Ratio
4
3
2
1
0
****
Ctrl
SEMA7A OE
Ctrl
OE

Figure 6

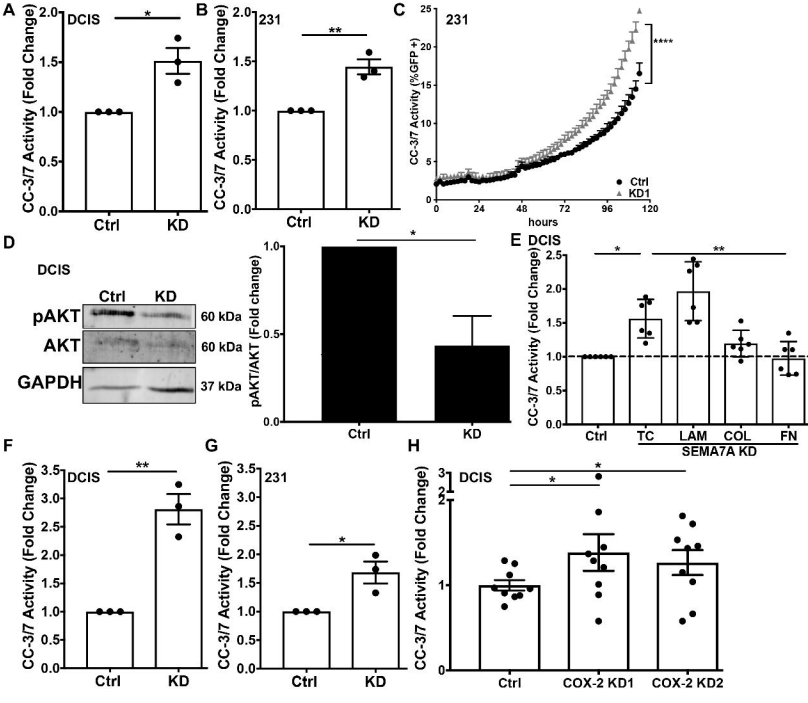
A
DCIS
CC-3/7 Activity (Fold Change)
Ctrl
KD
B
231
C
CC-3/7 Activity (%GFP+)
hours
Ctrl
KD1
D
DCIS
Ctrl
KD
pAKT
AKT
GAPDH
60 kDa
37 kDa
pAKT/AKT (Fold change)
E
TC
LAM
COL
FN
SEMA7A KD
F
G
H
COX-2 KD1
COX-2 KD2

Figure 7

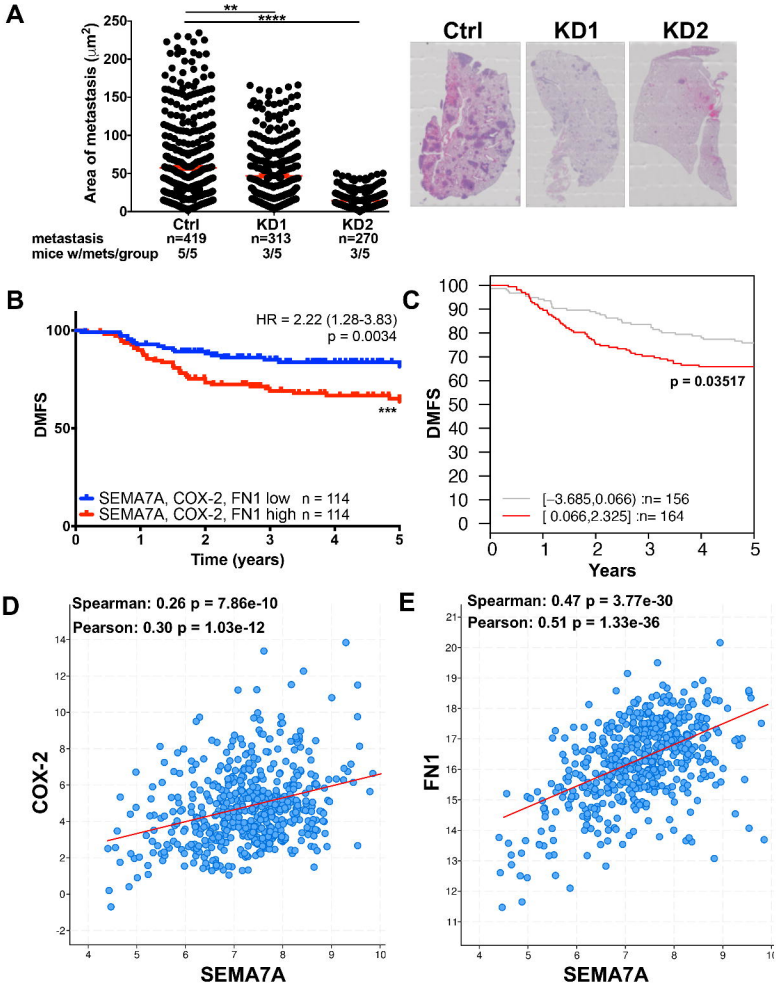
A
Area of metastasis (μm²)
**
****
Ctrl
KD1
KD2
metastasis
mice w/mets/group
Ctrl n=419 5/5
KD1 n=313 3/5
KD2 n=270 3/5
B
HR = 2.22 (1.28-3.83)
p = 0.0034
DMFS
***
SEMA7A, COX-2, FN1 low n = 114
SEMA7A, COX-2, FN1 high n = 114
Time (years)
C
DMFS
p = 0.03517
[−3.685,0.066) :n= 156
[0.066,2.325] :n= 164
Years
D
Spearman: 0.26 p = 7.86e-10
Pearson: 0.30 p = 1.03e-12
COX-2
SEMA7A
E
Spearman: 0.47 p = 3.77e-30
Pearson: 0.51 p = 1.33e-36
FN1
SEMA7A

Figure 8

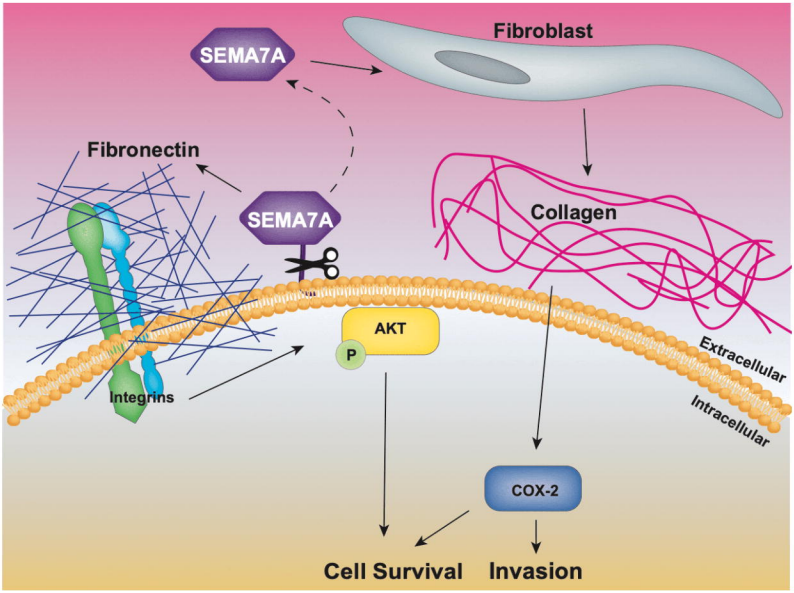
SEMA7A
Fibroblast
Fibronectin
SEMA7A
Collagen
AKT
P
Integrins
Extracellular
Intracellular
COX-2
Cell Survival
Invasion